Validating Validators: An analysis of DW-MRI Hardware and Software Phantoms

P. Rodrigues[1], V. Prckovska[1], W. L.P.M. Pullens[2], G. J. Strijkers[3], A. Vilanova[1], and B. M. ter Haar Romeny[1]
[1]Biomedical Image Analysis, Eindhoven University of Technology, Eindhoven, Noord Brabant, Netherlands, [2]Maatricht Brain Imaging Center, Maastricht University, Maastricht, Limburg, Netherlands, [3]Department of Biomedical Engineering, Eindhoven University of Technology, Eindhoven, Noord Brabant, Netherlands

INTRODUCTION: Diffusion Tensor Imaging (DTI) and its successor High Angular Resolution Diffusion Imaging (HARDI) are emerging MRI techniques for depicting *in-vivo* white brain matter anatomy and connectivity. HARDI and its ability to resolve more complex neural structures where DTI undoubtedly fails (i.e. crossing voxels) is thriving with new discoveries, but validation is still problematic. There is a wide range of utilizations of DTI and HARDI: from depicting the local structure of the probability density function of the water molecule displacement, fiber tracking, segmentation, etc. and the indispensable regularization schemes for the noisy local and global structures. However to apply any of the above-mentioned methods in a clinical setting, thorough validation is needed. The lack of knowledge about ground truth in brain white matter, leads to developments of artificial software images and the use of fiber phantoms. To our knowledge, there are two wide spread methods for creating artificial DWI data: the multi-tensor model and calculations based on the restricted diffusion inside a cylinder [1].

AIM: The goal of the present work is to validate DTI and HARDI software phantoms, in regions of either crossing fibers either single fiber bundles, in relation to measured phantom data [2] and *in vivo* data from human brain, acquired with identical parameters. Additionally, we address the noise issue, in DW-MRI, by applying Rician noise with realistic SNR, as calculated from the real data. Knowledge of the behavior of the synthetic data can improve the data modeling and processing and advance the employment of DTI and HARDI in clinical applications.

DATA: Multi-tensor (MT) model used in [3,4] and Soderman's (S) model [1] used in [5] for two fiber bundles crossing under 30˚, 50˚ and 65˚ were implemented in Mathematica. For the MT model we take the proportions of both fibers to be equal in the crossing areas, and the eigenvalues for each simulated tensor to be [300,300,1700]x10^{-6}mm^2/s. For the S model we use the same parameters for b value, Δ and δ, from the MRI acquisition protocol, and we average the signal values in the crossing areas. Both models use the same gradient sampling scheme as in the MRI scans of the *in vivo* and hardware phantom (#vols(#dirs): 132(120), 80(72) directions, each at b values of 1000, 2000, 4000 s/mm^2) and add Gaussian noise to the real and complex part of the signal with realistic SNR corresponding to the used b values (15.3, 13.3, 11.9 respectively). For the *in vivo* data we select a region of *corpus callosum* as linear part and known crossing between *corpus callosum* and *centrum semiovale*.

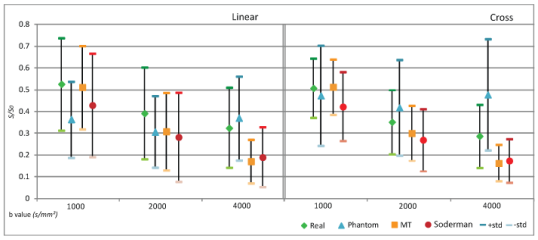

Figure 1. Average normalized signal values and standard deviations.

The software phantoms were generated in a synthetic dataset creation tool developed in Mathematica. The different fiber bundles in the volume are parametrically defined by specifying the centre line of the bundle, seen as a cylinder with a given radius. In each voxel of the volume, the respective fiber(s) orientation(s) is taken in order to simulate the respective signal attenuation. S model is of higher computational complexity than the MT model. In Mathematica, the signal attenuation for S model, 132 directions, n=1000, m=10 and k=10, requires approximately 30 minutes to compute, in a Tyan VX50 with 4 Dualcore Opteron 2.2Ghz CPU and 64GB of RAM. The MT model requires approximately 1 minute. This tool establishes an easy to use framework to generate datasets by simply defining lines by their parametric equations. As an example, this framework was also used to generate datasets for geodesics studies where U shaped fiber bundles, with torsion, are of great interest.

b value (s/mm²)		Linear				Cross			
		real	*phantom*	*MT*	*S*	*real*	*phantom*	*MT*	*S*
1000	*FA*	**0.80**	0.40	**0.80**	0.88	**0.37**	**0.43**	0.55	0.67
	MD	**0.0008**	0.0012	**0.0008**	0.0011	**0.0008**	0.0010	**0.0007**	0.0009
	Cl	**0.59**	0.21	**0.60**	0.71	**0.10**	**0.20**	0.27	0.37
	Cp	**0.14**	**0.15**	0.05	0.05	0.31	0.23	0.27	0.28
	K1	**0.0023**	0.0037	**0.0023**	0.0032	0.0023	0.0030	0.0021	0.0028
	K2	**0.0011**	0.0007	**0.0011**	0.0019	0.0004	0.0006	0.0006	0.0011
	K3	**0.94**	0.53	**0.99**	**0.99**	-0.37	0.29	0.52	0.68
	Ang. Diff	-	17.58	**1.61**	1.77	-	-	-	-
4000	*GA*	**0.44**	0.07	**0.49**	0.63	**0.18**	**0.08**	0.32	0.41
	FMI	0.16	1.25	0.22	0.26	**0.88**	**0.96**	0.26	0.26
	Ang. err;std	-	-	-	-	-	13.58;7.28	**10.15;5.34**	10.6;7.76

Figure 2. Summary of DTI and HARDI measures.

ANALYSIS: We model the HARDI data with Q-ball imaging and include Laplace Beltrami smoothing with λ =0.006 as in [4]. We apply wide range of DTI and HARDI scalar measures on the four different types of data. We also quantify the angular difference of the simulated linear direction and estimated main eigenvector in the DTI analysis, as well as the angular error and the standard deviation of the simulated and recovered ODF's angle.

RESULTS: In Fig.1 the average normalized signal values for the analyzed voxels in the different datasets in the linear and crossing part are summarized. Signal decay (as to be expected) with increasing b value is observed in most of the cases, and the signals of the S model converges towards the MT model at high b values. For clarity and simplicity, Fig. 2 displays the results of the average DTI and HARDI scalar measures for b equals 1000 and 4000 s/mm^2 only, b values which best depict the data's properties according to the used model. Given that the results for 80 and 132 gradient directions were essentially the same, we present only the latter and only the datasets with 65˚of crossing fibers since qualitatively they are the most similar to the selected region from the *in vivo* data. In [1] the signal for a crossing voxel is obtained by adding the contribution of both fiber populations. The results of the S model with added signals are not presented since they give too distinct results. For the HARDI measures we use only 4th order of the Spherical Harmonics coefficients calculated with the Q-ball model. The bolded results in Fig. 2 are the ones most similar to the real data. We observe similarity between the real and the MT model results. The results from the S model become similar to the *in vivo* ones at high b values, which can be useful in HARDI analysis, but for DTI analysis we recommend the MT model.

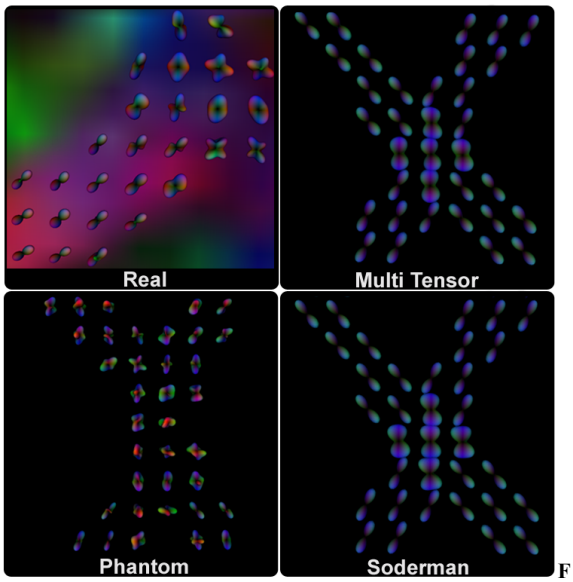

Figure 3. Q-ball glyphs with 4th order of Spherical Harmonics representation for the different datasets.

DISCUSSION&CONCLUSION: Analysis of different artificial DWI phantom data compared to real data is presented. Two different gradient sampling schemes and three different b values, applicable in clinical setting, were used. In most of the cases, the MT model exhibits similar behavior to the *in vivo* data. Another point in favor is its simplicity and low computational costs, which all together recommend it as a good choice for software synthetic generation. The results of the S model converge towards the ones from the MT and *in vivo* data for higher b values. The qualitative results (see Fig. 3) suggest that the noise level for the selected b values is much lower in the S and MT model than for the scanned data. Caution should be taken here, since only one specific region of crossing in the *in vivo* brain was analyzed and these results might vary in other selections. Future work will address different range of acquisition parameters and different selections of regions from *in vivo* data. The S model is frequently used for rat studies with high-field pre-clinical scanners, which allows for a significantly shorter δ as with a clinical scanner. Future work should investigate this type of real data and compare the behavior of the S model.

REFERENCES: [1] Soderman et al, MRM 1995; [2] Pullens et al, ISMRM 2007 [3] Descoteaux et al, MRM 2007; [4] Descoteaux et al, MRM 2006; [5] Ozarslan et al, NeuroImage 2006;